Chapter 5
Process Machine Interaction in Pendulum and Speed-Stroke Grinding

M. Weiß, F. Klocke, and H. Wegner

Abstract. The complex interaction of process forces and machine structure affects the quality of ground workpieces, especially in highly-productive machining processes, if machines are operated at their limits. In speed-stroke grinding, the highly-dynamic process forces are caused by high workpiece velocities and high acceleration of the machine table. These forces are influenced by the process parameters, the material properties, the coolant application and the grinding tool specification. The paper describes the approach to simulate the process machine interaction in speed-stroke grinding by a coupled model. The machine is modeled by a multi-body simulation, which can depict the static and dynamic behavior of the machine for every working position. This machine model is coupled with an analytical-empirical force model, which predicts the process forces regarding the process parameters, the coolant application and the workpiece material. The machine control system is implemented in the model as well. The ability to model a speed stroke grinding process, including the machine, the control system and the process itself can be used to predict and improve the workpiece quality regarding the measurement accuracy minimizing time and cost intensive experiments.

5.1 Introduction

In many cases, grinding is the only economical process to machine parts. Materials, which are especially difficult to machine, are ground to achieve high productivity and meet the requirements in terms of surface qualities. This paper focuses on speed-stroke grinding. Speed-stroke grinding is defined as a surface grinding process with high table speeds. The table speed of most of the conventional grinding machines is limited to 30 m/min. Pendulum grinding with table speeds higher than 50 m/min is defined as speed-stroke grinding [1]. In speed-stroke grinding the chip formation mechanisms change to bigger chips causing lower specific grinding energies at high table speeds. The resulting lower heat transfer to the workpiece can be used to improve the workpiece quality or the productivity of grinding processes. Speed-stroke grinding can be applied for machining highly heat-resistant materials and ceramics as well as hardened steel [2, 3, 4].

High table speeds result in short contact times between the grinding wheel and the workpiece. Short run-in and run-out phases lead to high gradients of process forces. The values of these forces are influenced by the complex interaction

B. Denkena and F. Hollmann (Eds.): Process Machine Interactions, LNPE, pp. 101–119.
springerlink.com

between the process parameters, coolant application and the mechanics of chip formation specific to the behavior of different workpiece materials. The material removal in grinding is realized by an amount of single grinding grits with an undefined shape. Several grinding grits are in contact with the workpiece surface at the same time, realizing material removal. Hence, it is a complex challenge to predict the forces occurring in the grinding process, their influence on the excitement of the machine structure and, thus, the workpiece quality.

In the following, an approach is shown, where the machine is modeled by a flexible multi-body simulation and the occurring forces by an analytical-empirical force model. These two models are coupled to comprehend the process-machine system. As an input for the simulation model and to validate the simulation results experimental investigations have to be conducted. The results of the analysis of the process and the machine behavior were used to set up the simulation model. Afterwards, experimental investigations of certain influences on the machine behavior and process forces resulted in a more detailed and more exact model of the whole process and lead to a potential of optimization for industrial pendulum and speed-stroke grinding processes.

5.2 Experimental Investigation

To realize a solid data base as an input for modeling the machine properties and the occurring process forces and vibrations have to be analyzed. The machine behavior is examined by a modal analysis of the used speed-stroke grinding machine. The influence of different materials, process parameters and coolant application on the process forces were examined by multiple grinding experiments with different setups, as described below.

5.2.1 Experimental Setup

For the experimental investigations a *BLOHM PROFIMAT 408 HTS* speed stroke grinding machine was used. In comparison to conventional surface grinding machines this machine is equipped with linear drives for the machine table movement. Thus, the workpiece velocity can reach up to $v_w = 200$ m/min. The table is driven with a maximum acceleration of $a_w = 50$ m/s^2. Because of the high table speeds and acceleration, especially at the reversal of the machine table, an impulse decoupling with spring-dampening elements and an eddy current brake is mounted beneath the machine table to reduce the impact on the structure and the process. The machine and the 3D CAD model of the machine interior are shown in Fig. 5.1. For the experiments, a precision height adjustment for coolant application was designed and mounted to the headstock. This allows a repeatable adjustment of different nozzles regarding the nozzle angle, axial position and height of the coolant application. Hence, it is possible to conduct experiments with defined coolant application parameters. For the experiments, the dynamic forces during pendulum and speed-stroke grinding processes were measured by a multi-component force dynamometer.

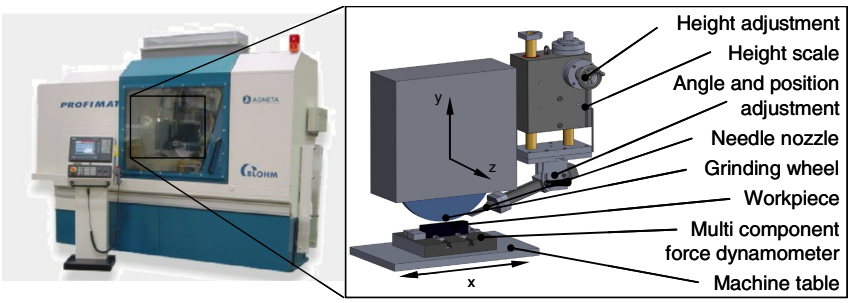

Fig. 5.1 CAD drawing of machine interior with precision nozzle height adjustment

The static and dynamic behavior of the machine was examined by an experimental modal analysis of the machine tool. A hydraulic actor unit was mounted to the machine. This actor unit applied dynamic loads with different frequencies to the grinding wheel. A piezo-electric sensor unit measured the response of the machine structure to the dynamic loads. This procedure was repeated with different sensor and actor positions in x, y and z direction so that the cross relations between the excitations could be measured. More information about modal analysis can be found in Section 1.2 of this book. The data was used to parameterize the machine model. Thus, a comparison between the modeled and the real machine behavior can be carried out.

5.2.2 Experimental Results

In the following, the results of the experiments are shown. At first, the measured machine behavior is described. The results of the grinding experiments and the evaluation of occurring grinding forces are shown below.

Modal analysis of machine behavior

As a basis for the research of the interaction of the machine and the grinding process the static and dynamic machine behavior needs to be determined. The frequency response function of the used machine is shown exemplarily in Fig. 5.2. The static and dynamic load is induced in y-direction as well as the measured deflection. Variations of the tool centre point in y-direction are causing deviations in dimension of the ground workpiece as they are influencing the depth of cut instantaneously. The system was preloaded with a force of 1,000 N. Measurements show that the static elasticity of the machine is 0.03 µm/N. The first three eigenfrequencies are at 38, 58 and 78 Hz with maximum amplitude higher than the static flexibility. A modal analysis was conducted to identify the eigenmodes of the system. The results and the comparison with the modeled machine behavior are shown in the chapter Modeling and Simulation.

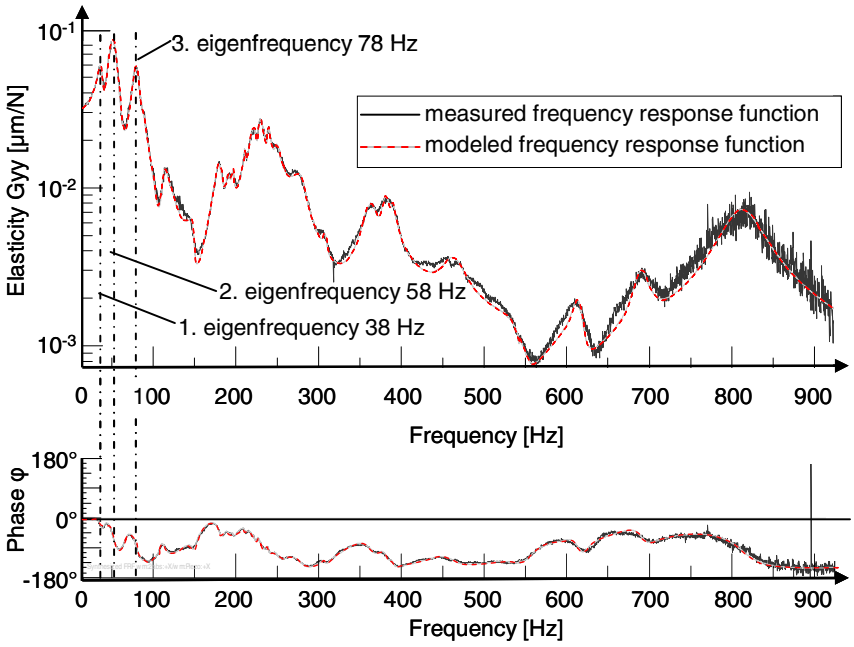

Fig. 5.2 Frequency response function (Gyy) of test machine, preload 1,000 N

Process forces

In the experiments, the dynamic forces during pendulum and speed stroke grinding processes are measured by a multi-component force dynamometer and recorded on a PC. The measurement of specific normal and tangential forces and the acoustic emission (AE) signal during two passes of the grinding wheel is shown in Fig. 5.3. It was recorded in the middle of a speed-stroke process at a ground volume of $V'_w = 500$ mm^3/mm. The AE-signal is important for the analysis of the data. Every time the grinding wheel gets in contact with the workpiece a peak in the AE-signal can be detected. Thus, the exact time frame from the first to the last contact of the grinding wheel with the workpiece can be specified.

To explain different effects the measurement is separated into nine phases. At the beginning of Phase 1 the workpiece is on the left side of the machine and accelerates towards the grinding wheel. Because of the moment of inertia the specific tangential forces show a characteristic peak during the acceleration. At the beginning of Phase 2 the workpiece is engaged by the grinding wheel. With a workpiece velocity of $v_w = 80$ m/min and a depth of cut $a_e = 15$ µm the run-in time is very short. It takes less than 2 ms from the first contact of the grinding wheel until the maximum depth of cut is reached. However, the normal force needs a certain time to reach its stationary level at the end of phase 2.

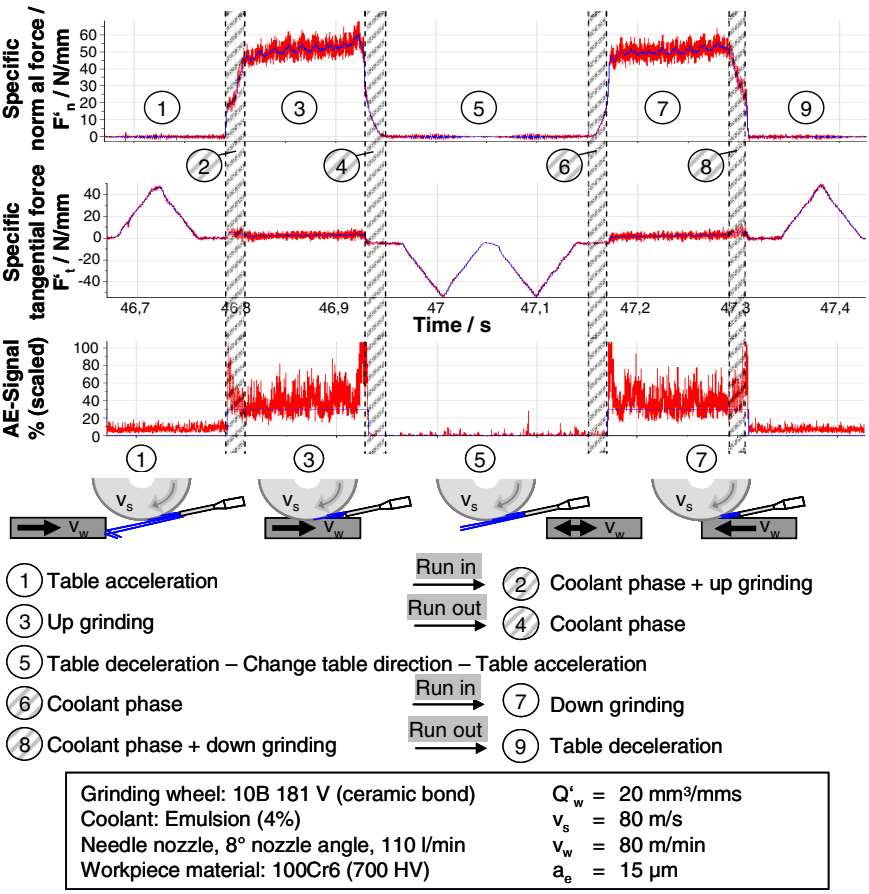

Fig. 5.3 Force and acoustic emission signals during speed-stroke grinding

Responsible for this effect is the coolant. With the shown machine setup the coolant nozzle is on the right side of the grinding wheel. If the workpiece is approaching from the left side, the main coolant flow is not able to get into the contact zone. The coolant jet hits the workpiece from the right side. Until the workpiece moves further the coolant jet builds up a hydro-dynamic pressure in and in front of the contact zone, as described in [6, 7]. Depending on flow rate, coolant speed, nozzle angle, nozzle position and process parameters the coolant adds a significant value to the normal force [8]. Besides that, the hydrodynamic coolant pressure influences the dampening behavior of the system [9].

During phase 3 the process is nearly stationary. At the end of this phase, the normal forces drop rapidly because of the disengagement of the grinding wheel. After this, the coolant forces drop with a time delay in phase 4. As the gap

between the workpiece and the grinding wheel gets wider while the workpiece moves apart the measured normal force decreases. In phase 5, the workpiece table decelerates, changes its direction and accelerates in the opposite direction, which can be seen in the tangential force progression. Phase 5 shows that the level of acoustic emission is lower than in phase 1 and 9 even though the grinding wheel is not in contact with the workpiece. The reason for this phenomenon is that the coolant jet hits the workpiece from the side during phase 1 and 9. When the grinding wheel is at the right side of the grinding wheel there is no coolant splashing against the workpiece.

Phase 6 is characterized by an increase of normal forces while the workpiece is not in contact with the grinding wheel yet. This is related to the dynamic coolant forces, which build up because of the narrowing gap between the workpiece and the grinding wheel. The run-in takes place at the beginning of phase 7. Before the workpiece runs out of contact the forces drop as a result of the deflected coolant jet.

The described effects show the complexity of forces occurring during the grinding process. To model the forces the main influences have to be taken into consideration. In order to quantify the effects of process parameters workpiece material and coolant application numerous systematic experiments have been conducted.

The measured force signal contains a lot of information about the process and the influences mentioned above. To separate the effect of the chip formation from the coolant induced forces the data has to be analyzed as shown in Fig. 5.4. On the upper left, measured specific normal forces plotted against the grinding wheel circumferential speed v_s up and down grinding are shown. The forces drop with higher rotation speed of the grinding wheel from above 30 N/mm to 20 N/mm.

The coolant forces were measured after every fifth stroke of the process by conducting one stroke without a depth of cut a_e. The results are shown exemplarily in Fig. 5.4 on the upper right. The coolant induced forces increase up to a certain point – here 80 m/s – before they begin to decrease at higher circumferential speeds. For conventional processes a similar trend was described by Heinzel [10]. Higher grinding wheel circumferential speeds lead to a higher flow rate through the contact zone. Hence, less coolant ponds in front of the contact zone and the pressure in this area drops. As a result, the specific coolant normal forces decrease.

If the specific coolant normal forces F'_{nKSS} are subtracted from the measured specific grinding normal forces F'_n, the specific cutting normal forces $F'_{c,n}$ can be identified. This is necessary to evaluate the separate effects and to simplify the modeling of the occurring forces in grinding as every effect can be examined separately.

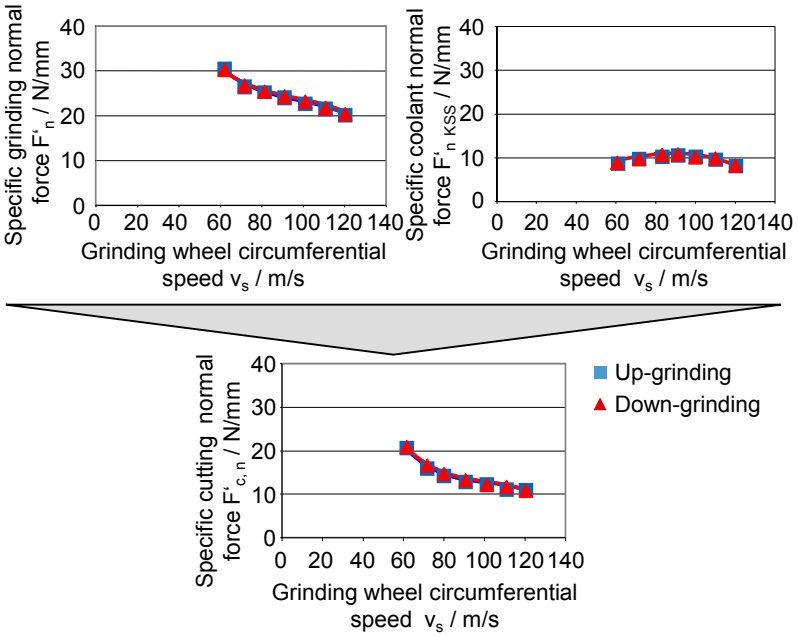

Material:	**Grinding parameters:**	**Coolant application:**
100 Cr 6 (AISI 52100)	v_w = 120 m/min	Oil
Grinding wheel:	a_e = 10 µm	Needle nozzle, 11°
CBN 10B 181 V	Q'_w = 20 mm³/mms	Flow rate: 62 l/min

Fig. 5.4 Evaluation of cutting and coolant-induced forces

Besides the hydrodynamic pressure, which builds up in and in front of the contact zone, additional coolant forces can be induced due to the ground geometry. An example is shown in Fig. 5.5. Narrow gaps between parts of the grinding wheel, which are not in contact with the workpiece, and the workpiece lead to additional hydro-dynamic forces. The smaller the gap, the higher these forces. If such workpiece geometries are ground, the additional coolant forces need to be considered.

In addition to the forces, the coolant has an influence on the dampening behavior of the whole process machine system. To evaluate these effects the following experimental setup was used. A workpiece made up of the two different materials is ground. On one side, the workpiece consists of hardened 100Cr6 and on the other side of *Ureol*, an easy to machine and homogenous modeling material. This workpiece was ground with high table speed. The machining of the modeling workpiece material creates very small forces compared to the bearing steel.

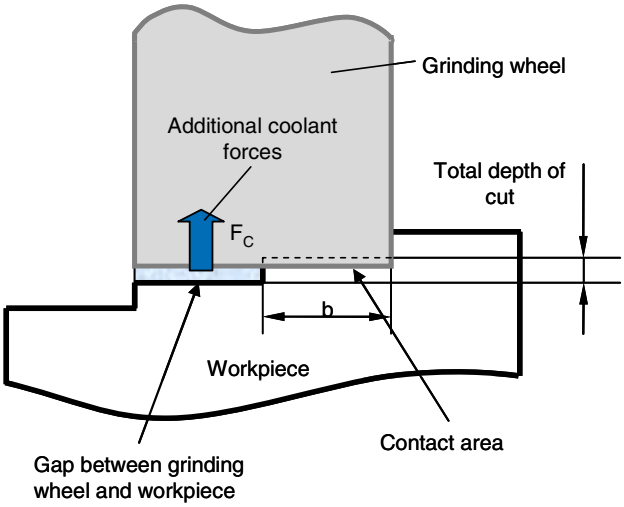

Fig. 5.5 Additional coolant forces by means of workpiece geometry

The experimental setup is shown in Fig. 5.6. As a result, the forces drop rapidly at the junction of the two materials. If no coolant is used, a deviation of the profile height can be measured on the surface of the soft material. When using coolant the deviation is much smaller due to dampening and pre-load effects of the fluid in and in front of the contact zone. Although several experiments with this setup were accomplished quantitative statements about the dampening behavior could not been derived yet as the collected data scatters in a big range. As a consequence, the experimental setup and measurement need to be improved.

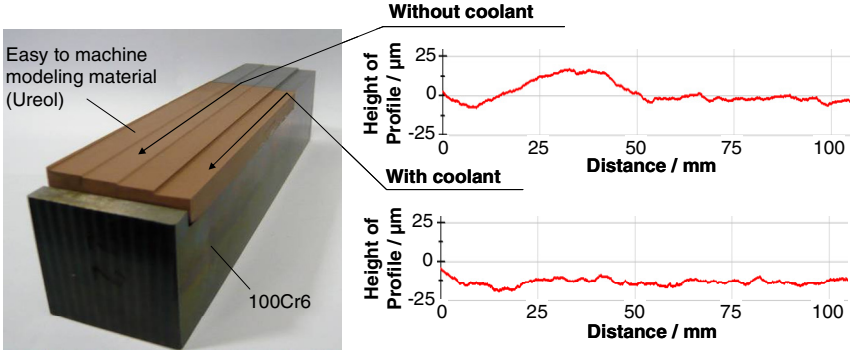

Grinding wheel: 10B 181 V	Q'_w = 20 mm³/mms
Coolant: Emulsion (4%)	v_s = 90 m/s
Needle nozzle, 8° nozzle angle, 110 l/min	v_w = 120 m/min
Workpiece material: 100Cr6 (700 HV)	a_e = 10 µm

Fig. 5.6 Influences of coolant dampening and pre-load effects

Another important influence on the occurring forces is the workpiece material. Experiments have been conducted with the aim of evaluating the process forces grinding different materials with speed-stroke grinding parameters. As an example, the specific normal forces depending on the hardness of the material and the table speed are shown in Fig. 5.7. Smaller chip thicknesses at low table speeds lead to more friction and forming processes in chip formation compared to higher table speeds. Thus, the specific grinding forces are lower at high table speeds [11]. The effect of the material hardness on the specific normal forces decreases with higher table speeds. For certain groups of workpiece materials, this kind of modeling is sufficient. However, there are different effects on the grinding forces regarding different workpiece materials. As shown in the figure, the specific normal forces are higher while grinding the ductile and tough nickel-based alloy Inconel 718 at different table speeds compared to 100Cr6. Hence, a force model needs to be adapted to different workpiece material properties. Composition and structure of the workpiece material are the main influences on the grindability of workpiece materials. Furthermore, the workpiece temperature has an influence on the machinability. The necessary force to form a chip decreases at higher temperatures but as the energy flow to the workpiece is comparatively low in speed-stroke grinding this effect is neglected in the following model.

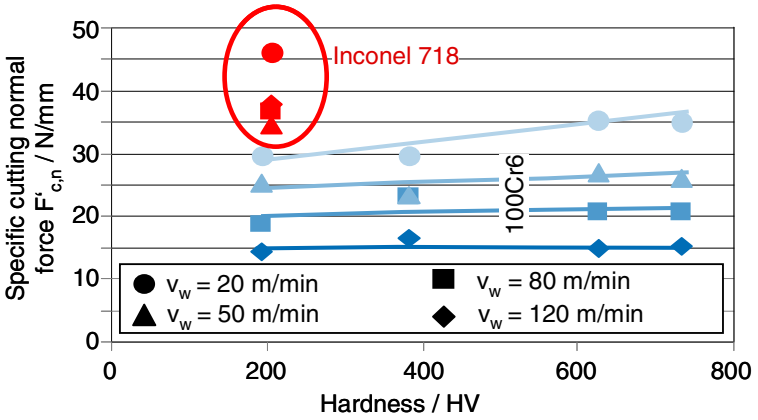

Material:	**Grinding parameters:**			**Coolant application:**
100 Cr 6 (AISI 52100) and Inconel 718	v_s	=	120 m/s	Emulsion 4 %
Grinding wheel:	a_e	=	60, 24, 25, 10 µm	Needle nozzle (11°) + clearing nozzle
CBN 10B 181 VP	Q'_w	=	20 mm^3/mms	Flow rate: 110 l/min

Fig. 5.7 Specific cutting normal forces grinding different materials

The material removal in grinding results from various contacts between the grinding wheel and the workpiece. In addition, the grinding grits have irregular shapes and they move on a certain path around the centre of the grinding wheel. Because of this, some of the grits just plow through the workpiece surface, some grits form chips and some are not in contact with the workpiece surface. A large

amount of the energy is transferred into elastic and plastic deformation of the workpiece material. Hence, the grinding wheel properties, depending on influences like grit size, bond type or dressing conditions, influence the occurring forces significantly. Different grinding wheels were tested and need to be implemented in the modeling as well, as shown in the following chapter.

5.3 Modeling and Simulation

To model the complex interaction between the machine and the process with the highly dynamic forces shown in the chapter above an approach with a coupled model is used. The model is implemented in Matlab Simulink and calculates the forces and deviations in discrete time steps. The first part of the model is the machine, which is represented by a moveable multi-body simulation (MBS). The occurring grinding forces are predicted by an analytical-empirical process model. These forces are calculated and transferred to the machine model. Due to the elasticity of the machine these forces lead to a deviation of the tool centre point and thus to a deviation of the ground workpiece shape. These deviations are transferred to the force model, where the forces for the following time step are calculated. The model operates in discrete time steps, which are arbitrary in the simulation. Another important part of the model is the simulation of the machine control system as the response time of the control system can lead to deviations in speed-stroke grinding processes as well. The principle of the coupled simulation is shown in Fig. 5.8. Coupled simulations permit the usage of different simulation environments with data exchange by means of a suitable interface. Proper interfaces have to be designed [12]. Another advantage of coupled models is the possibility to adapt each of the models separately so that changes and improvements can be carried out more easily.

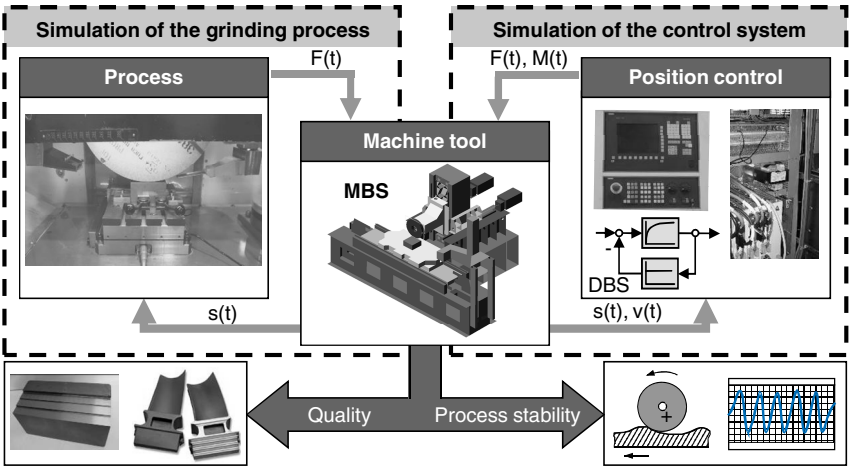

Fig. 5.8 Coupled process – machine – control simulation

For the designed model the simulation of the process forces and the control system is implemented into Matlab Simulink. In the following, the machine and the process model are described in more detail.

Machine model

For the design of a MBS model of a machine the following steps have to be conducted. The procedure of the development of a MBS machine model is shown in Fig. 5.9.

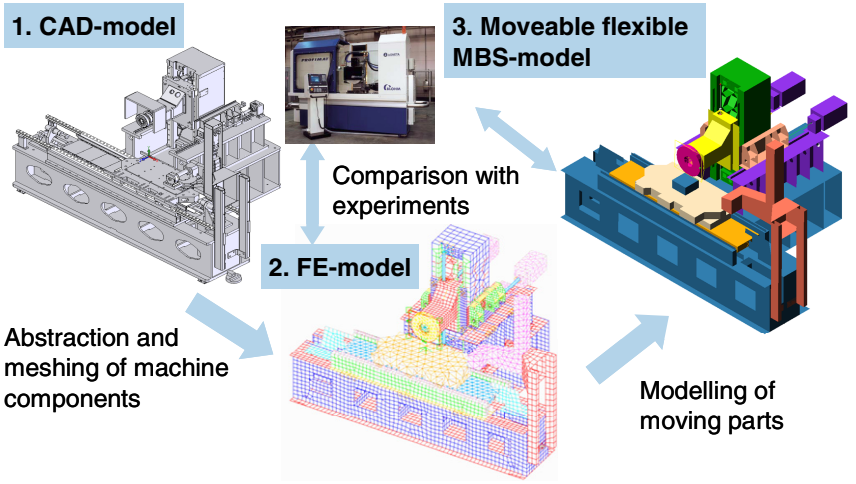

Fig. 5.9 Procedure for the development of a multi body machine model

Based on CAD data of the machine the relevant parts need to be abstracted. Small bore holes and small radii are removed because they have no significant influence on the stiffness or the mass of the system. As a result, the FE-meshing of the finite element model (FE-model), which is performed afterwards, is less complex. Next, guiding systems, spindle bearings and screw connections are approximated by simple spring elements. Afterwards, a comparison between the measured machine behavior and the simulated machine is conducted to evaluate the required stiffness of the joints. Furthermore, the relevant eigenmodes and eigenfrequencies can be depicted. Fig. 5.10 shows the 2nd eigenmode of the machine system at 58 Hz exemplarily.

For the MBS-model the FE structure parts have to be converted into flexible bodies. A flexible body allows the description of its flexible properties at defined force transmission points. The calculation of the forces at these knots and the elastic deformation of the parts is implemented in MSC.Adams and calculated by a developed sub-routine for every position of the spindle and the machine table in the machine. The special aspect about the developed MBS-model is the possibility of realizing a movement of certain parts. This allows the simulation of movements of the spindle and the machine table like in the real machine. More detailed information about the machine model and the subroutines can be found in [13, 14].

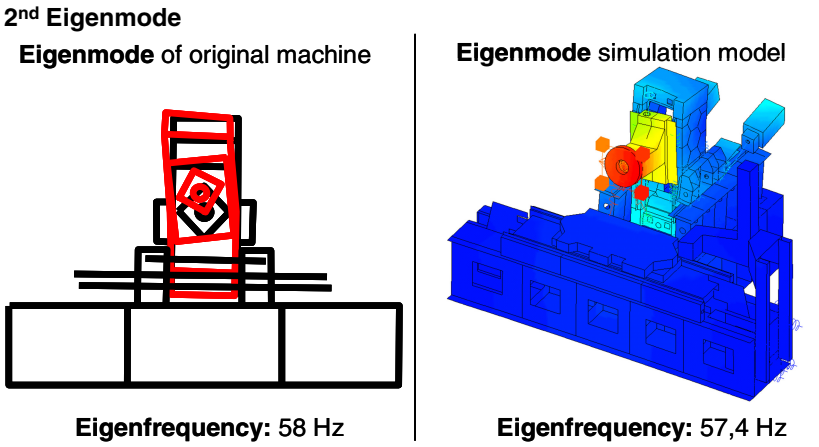

Fig. 5.10 Comparison between measured and simulated eigenmode and eigenfrequency

Moveable MBS-models have the advantage of representing the machine behavior for every position of the machine components. However, the design of a moveable MBS-model of a machine is very time consuming and a lot of knowledge about the machine structure and the stiffness of the joints is necessary.

Process model

The task of the process model is to calculate the occurring forces during the grinding process, regarding the position of the grinding wheel, the grinding parameters and other boundary conditions. Many grinding force models have been developed over the last decades. Usually, a technological study of grinding processes results in the development of a model, which is valid for a closely limited field with given boundary conditions, as grinding is a very complex process of material removal [15]. Many models to predict the grinding forces are presented in [15, 16, 17]. Most of these models consider the kinematic of the grinding process and an empirical additive, which represents the influences of the grinding wheel and the workpiece material.

For the prediction of the grinding forces during speed-stroke grinding an adapted grinding force model was developed. The schematic representation of the model is shown in Fig. 5.11. Depending on the workpiece position the current material removal is calculated by using a chip longitudinal section A_l, which represents the intersection of the grinding wheel and the workpiece during one time step of the simulation. This longitudinal section A_l is multiplied by an experimental investigated force-ratio factor, which is dependent on the process

parameters, the material properties and the grinding wheel specification, to get the cutting forces. Simultaneously, the coolant forces are calculated. These forces are dependent on the workpiece position and the process parameters as well, which was shown before. Additionally, coolant application parameters like nozzle angle, nozzle type and coolant flow rate are considered [18]. The coolant forces and the cutting forces are summarized to the total process forces.

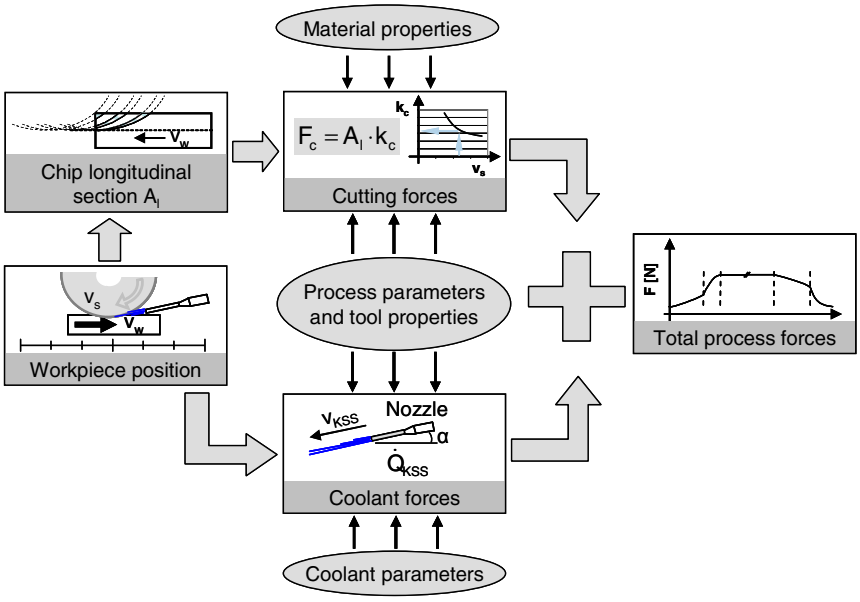

Fig. 5.11 Schematic representation of the force model

In the following, the single modeling steps are described in more detail. Fig. 5.12 shows the calculation of the chip longitudinal section during the run-in phase. In position I, the grinding wheel first gets into contact with the workpiece. During the run-in phase the contact length increases and thus the material removal per time step also increases. This increasing material removal is proportional to the area, which is bordered by the contact length between two time steps. Towards time step III the maximum depth of cut is reached and the chip longitudinal section does not change in case of an even workpiece surface. Grooves in the workpieces can also be represented by the model.

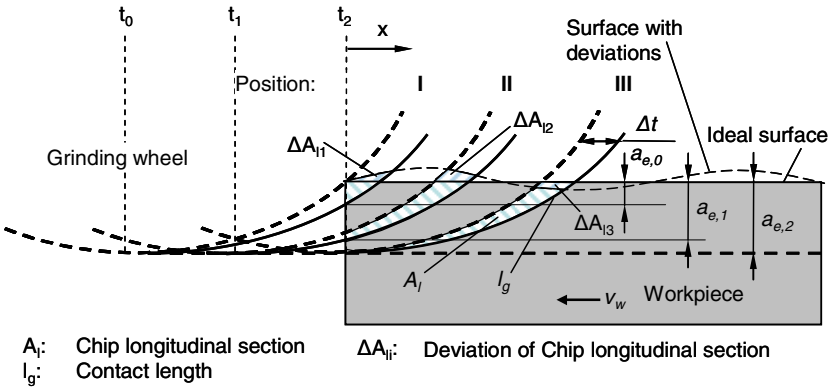

Fig. 5.12 Chip longitudinal section during run-in of the grinding wheel

With constant time steps Δt the change of the longitudinal chip section can be described by geometrical values. For a constant workpiece velocity v_w the longitudinal chip section can be described as a function of the position x according to equation 1 during the run-in phase.

$$A_{l,\text{Run-In}}(x) = -\frac{A_{l,\max}}{l_g^2}x^2 + \frac{2 \cdot A_{l,\max}}{l_g}x \pm \Delta A_{li} \tag{1}$$

$A_{l,max}$ is the maximum chip longitudinal section, which is reached after the run-in of the grinding wheel at the maximum depth of cut a_e. ΔA_{li} is the deviation of the chip longitudinal section A_{li} due to an uneven surface or the geometry. At the run-out, the chip longitudinal section is calculated with the following equation:

$$A_{l,\text{Run-Out}}(x) = \frac{A_{l,\max}}{l_g^2}x^2 - \frac{2 \cdot A_{l,\max}}{l_g}x + A_{l,\max} \pm \Delta A_{li} \tag{2}$$

If the workpiece has no deviations at the surface, the chip longitudinal section stays constant. Fig. 5.13 shows the cutting force characteristic of one stroke during grinding. In speed-stroke grinding, the run-in and run-out phases are in the range of milliseconds. If the table speed is 120 m/min at a depth of cut of 10 µm, these phases take 0.935 ms, for example. If there are deviations in the surface, an additional ΔA_{li} needs to be added for the calculation.

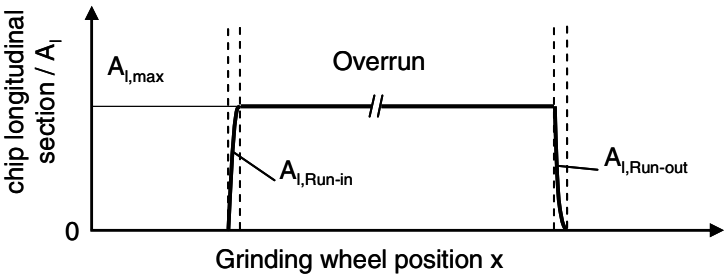

Fig. 5.13 Characteristics of total chip longitudinal section during one stroke

By modeling the chip longitudinal section it is possible to calculate the intersection between the grinding wheel and the workpiece for surface grinding processes [19]. This is equivalent to the actual material removal, taking the depth of cut and the workpiece velocity v_w into account. Uneven workpiece surfaces lead to a changing material removal, which is also considered in the model. In unfavorable cases, the change of the material removal rate in one stroke can lead to chatter effects. This could be provoked neither during the grinding experiments nor in the simulation. This result corresponds to the modal analysis shown in chapter 2 as there are no distinct weaknesses of the machine regarding chatter effects.

To predict the forces, which affect the machine structure quantitatively, the modeling focuses on the process parameters, the workpiece material and the coolant as these influences were emphasized as the significant influences in speed-stroke grinding. First, the forces, which depend on the process parameters, are calculated. The calculation of the forces is carried out by multiplying the chip longitudinal section with the determined force ratio factors k_c (Equation 3). The chip longitudinal section is dependent on the deph of cut a_e, the workpiece velocity v_w and the chosen time step Δt, as explained above. The influences on the force ratio factor k_c are the grinding tool, the material properties, e. g. the hardness and the sort of material, and the grinding wheel circumferential speed v_s.

$$F_i = A_l(a_e, v_w, \Delta t) \cdot k_c(v_s, Material, Tool) \tag{3}$$

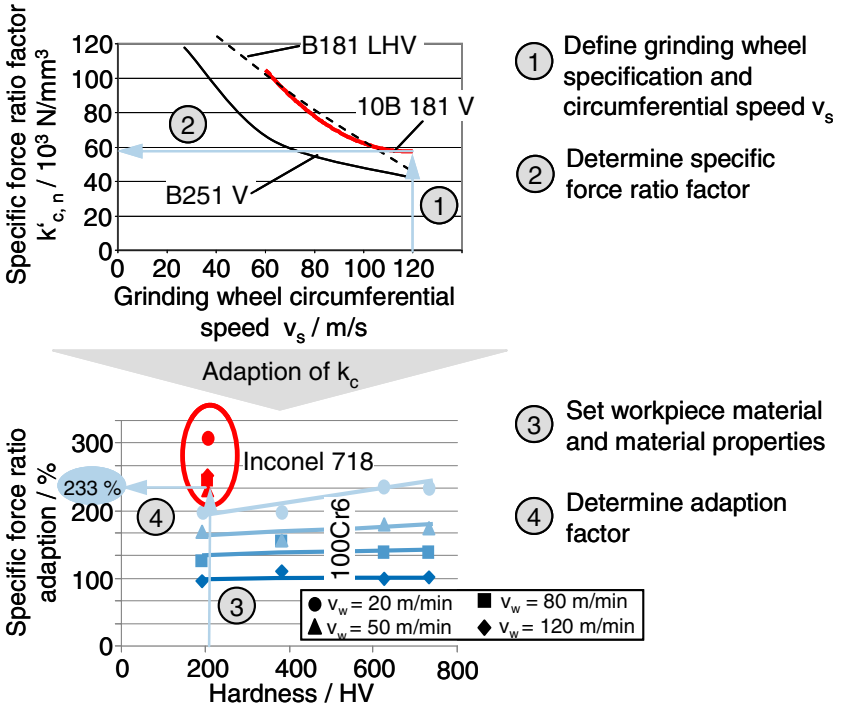

Fig. 5.14 Adaption of force ratio factor k_c

As the different influences are taken into account the k_c factor has to be adapted. An example for the functionality of the model is shown in the following. Fig. 5.14 illustrates the calculation of the adapted force ratio factors. Different grinding wheel specifications lead to specific force ratio factors k_c at different circumferential speeds v_s. The data was generated in several experiments for different grinding wheels. In the example in Fig. 5.14, a grinding wheel with a grit size of 181 µm is used.

The first diagram at the top of the Figure shows the determination of the specific force-ratio factor for a vitrified, bonded CBN wheel with a grit size of 181 µm at a circumferential speed of 120 m/s. The specific force-ratio factor is 59,000 N/mm^3, assuming defined standard conditions. These standard conditions are hardened and tempered 100Cr6 as the workpiece material and a combined needle nozzle with a clearing nozzle with a total coolant flow rate of 110 l/min. After the "standard" force-ratio factor k_c has been calculated it needs to be adapted by the influences mentioned above. In the example in Fig. 5.14, the nickel base alloy Inconel 718 is chosen. As mentioned above, the material, which is difficult to machine, leads to higher cutting forces. Thus, the force-ratio factor is adapted. In this case, the forces are higher by a factor of 2.33. This leads to a total specific force-ratio factor $k_{c,tot}$ of 137,470 N/mm^3.

The coolant application affects the forces in two ways. On the one hand, the coolant application has an influence on the chip formation, which leads to varying forces. This is also considered by an adaption of the force ratio factor k_c. On the other hand the hydrodynamic pressure adds a value to the total forces. The simulation program calculates these forces depending on the actual coolant conditions. The coolant forces are calculated in the model by using the workpiece position as the input factor as well. In combination with the process parameters and the coolant application, parameters like coolant flow rate and nozzle angle, the occurring forces can be predicted similar to the cutting forces. These are the most important parameter adjustments for the coolant supply [20].

In a last step, the total process forces for the current time step are summarized. Then the value is transferred to the machine model, which calculates the static and dynamic displacement of the grinding wheel. With the displacement, the cycle starts again with the calculation of the forces for the next time step. Hence, it is possible to record the tool path and the resulting surface.

A comparison between a measured and simulated surface is shown in Fig. 5.15. The measurement shows the characteristic super-elevation at the beginning. The fast-run in of the grinding wheel results in a rapid raise of the process forces. On this side of the workpiece, the system is pre-loaded by the hydrodynamic coolant forces. Accordingly, the profile height on the left side is higher at this side compared to the right. After a short period of vibration the workpiece is quite even. The peak in the middle of the measurement of the real surface is used as a reference as the measurement length of the used surface measurement device is less than 100 mm. On the right side of the workpiece the profile height drops. This is related to the decreasing coolant force at the right side of the workpiece, as described above. The height of this step varies depending on the process parameters and coolant application.

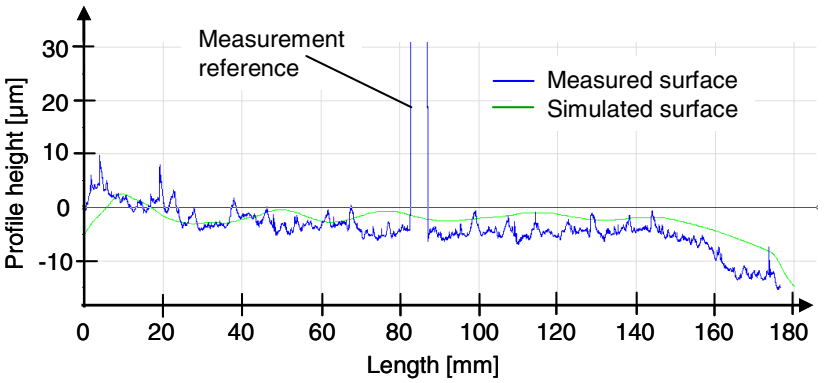

Material:	**Grinding parameters:**	**Coolant application:**
100 Cr 6 (AISI 52100)	v_s = 120 m/s	Emulsion 4 %
Grinding wheel:	a_e = 10 µm	Needle nozzle, 11°
CBN 10B 181 V	Q'_w = 20 mm³/mms	Flow rate: 62 l/min

Fig. 5.15 Measured and simulated workpiece surface after speed-stroke grinding

5.4 Optimization

The approach to model the interaction between the speed-stroke grinding process and the machine structure, as shown in this paper, can be used to improve production processes. Furthermore, it builds the foundation for further research for the understanding of the grinding process, especially speed-stroke grinding.

It was shown that the coupled simulation allows the prediction of the shape of the speed-stroke ground workpiece, taking the process parameters, the coolant application and the workpiece material into account. If the process result can be predicted without conducting time and cost-consuming experiments, a faster start of production can be realized. With the knowledge of the maximum deviation of the workpiece measurements the process time can be optimized. The roughing process leads to a certain surface. The grinding minimum allowance for the finishing strokes can be determined and, thus, the minimum cycle time can be depicted.

The developed coupled simulation can be adapted for other grinding processes. On the one hand, the grinding force model needs to be adapted for different grinding processes. In particular, the calculation of the current material removal rate needs to be adapted to other kinematics. On the other hand, a new machine model has to be built up for other machines. Depending on the process reduced machine models with less build-up effort may be sufficient. The advantage of flexible multi-body simulations is the ability to simulate the machine behavior in every position of the machine slides, the modeling effort, however, is very high, which is shown above. In a lot of surface grinding processes the spindle moves within a limited area in the machin only. As a consequence, the simulation of the machine by means of a multi-mass spring system can be sufficient. This system can be established in a substantially shorter time frame.

Another way to use the results of this work is to already evaluate the behavior of machines in the design phase. Based on the CAD data the machine can be modeled and the process behavior as well as the process result can be estimated without building and testing the new machine. Structural weaknesses and illegitimate process parameters can be determined, specific to the grinding processes.

5.5 Conclusion and Outlook

In speed-stroke grinding, the highly dynamic process forces cause deviations of the machine structure. In this paper, the development of a coupled process-machine model has been presented. An approach for modeling the process forces depending on process parameters, material properties and coolant application parameters has been described. The different effects, which influence the occurring process forces, have been analyzed separately in various experiments. Coupled with the MBS-model of the machine and the control system model the simulation is able to predict the workpiece quality in terms of measurement and form deviations.

In addition, the presented results have revealed potential fields of research in modeling the speed-stroke grinding process. In this project, only simple workpiece geometries were analyzed. Theoretically, the prediction of more complex geometries is possible. Another important issue is the influence of different coolant applications on the dampening behavior of the process machine system. From the conducted experiments, no distinct statement regarding this influence can be made.

A major goal of modeling production processes must be the evaluation of process results without time and cost-consuming experiments. At the moment, these experiments are still necessary to parameterize the developed models. The approaches developed in the priority program 1180 can be used as a basis for further research to understand the complex grinding process.

References

[1] Duscha, M., Klocke, F., D'Enremont, A., Linke, B., Wegner, H.: Investigation of Temperatures and residual stresses in speed-stroke grinding via Fea Simulation and practical tests. In: Proceedings in Manufacturing Systems, vol. 5(3), pp. 143–148 (2010)

[2] Zeppenfeld, C.: Schnellhubschleifen von gamma-Titanaluminiden. Gamma-Titanaluminiden. RWTH Aachen University, Aachen (2005)

[3] Nachmani, Z.: Randzonenbeeinflussung beim Schnellhubschleifen. Dissertation, RWTH Aachen University, Aachen (2008)

[4] Uhlmann, E., Sammler, C.: Schnellhubschleifen von Hochleistungswerkstoffen. Jahrbuch Schleifen, Honen, Läppen und Polieren, vol. 64, pp. 155–168. Vulkan-Verlag, Essen (2010)

[5] Weck, M.: Dynamisches Maschinenverhalten bei der Zerspanung mit undefinierter Schneide. Werkzeugmaschinen 5 – Messtechnische Untersuchung und Beurteilung, pp. 326–362. Springer, Berlin (2001)

[6] Beck, T.: Kühlschmierstoffeinsatz beim Schleifen mit CBN. Dissertation, RWTH Aachen University, Aachen (2002)
[7] Wittmann, M.: Bedarfsgerechte Kühlschmierung beim Schleifen. Dissertation, University of Bremen, Bremen (2007)
[8] Brinksmeier, E., Heinzel, C., Wittmann, M.: Friction, Cooling and Lubrication in Grinding. Annals of the CIRP, Keynote Paper 48(2), 581–598 (1999)
[9] Marksoud, T.M.A., Mokbel, A.: Suppression of chatter in grinding using high-viscosity coolants. Proceedings of the Institution of Mecanical Engineers, Part B (Journal of Engineering Manufacture) 216, 113–123 (2002)
[10] Heinzel, C.: Methoden zur Untersuchung und Optimierung der Kühlschmierung beim Schleifen. Dissertation, University of Bremen, Bremen (1999)
[11] Klocke, F.: Process Design. Manufacturing Processes 2 – Grinding, Honing, Lapping, pp. 251–287. Springer, Berlin (2009)
[12] Esser, M., Brecher, C., Witt, S.: Interaction of manufacturing process and machine tool. Annals of the CIRP, Keynote Paper 58, 588–607 (2009)
[13] Hoffmann, F.: Optimierung der dynamsichen Bahngenauigkeit von Werkzeugmaschinen mit der Mehrkörpersimulation. Dissertation, RWTH Aachern University, Aachen (2008)
[14] Klocke, F., Brecher, C., Sitte, B., Weiß, M.: Analyse der dynamischen Wechselwirkungen bei Pendel- und Schnellhubschleifprozessen. Jahrbuch Schleifen, Honen, Läppen und Polieren 64, 53–65 (2010)
[15] Tönshoff, H.K., Peters, J., Inasaki, I., Paul, T.: Modelling and Simulation of Grinding Processes. Annals of the CIRP, Keynote Paper 41(2), 677–688 (1992)
[16] Brinksmeier, E., et al.: Advances in Modeling and Simulation of Grinding Processes. Annals of the CIRP, Keynote Paper 55(2), 667–696 (2006)
[17] Aurich, J.C., Biermann, D., Blum, H., Brecher, C., Carstensen, C., Denkena, B., Klocke, F., Kröger, M., Steinmann, P., Weinert, K.: Modelling and simulation of process: machine interaction in grinding. In: Production Engineering – Research and Development, vol. 3(1), pp. 111–120. Springer, Heidelberg (2009)
[18] Weiß, M., Klocke, F., Wegner, H.: Influence of coolant and workpiece material properties on dynamic grinding forces in speed stroke grinding. In: Proceedings of the 2nd International Conference on Process Machine Interaction, Vancouver, G4 (2010)
[19] Klocke, F., Duscha, M., Hoffmann, F., Wegner, H., Zeppenfeld, C.: Machine – Grinding Wheel –Workpiece Interaction in Speed-Stroke Grinding. In: Proceedings of the 1st International Conference on Process Machine Interaction, Hannover, pp. 259–266 (2008)
[20] Wittmann, M., Heinzel, C., Brinksmeier, E.: Evaluating the Efficiency of Coolant Supply Systems in Grinding. In: Production Engineering – Research and Development, Braunschweig, vol. XI(2), pp. 39–42 (2004)